Supporting Information

High-Performance On-Chip Supercapacitors Based on Mesoporous Silicon Coated with Ultrathin Atomic-Layer Deposited In_2O_3 Films

Bao Zhu, [†, ‡] Xiaohan Wu, [†] Wen-Jun Liu, [†] Hong-Liang Lu, [†] David Wei Zhang, [†] Zhongyong Fan, [‡] Shi-Jin Ding [*, †]

[†] School of Microelectronics, Fudan University, Shanghai 200433, PR China

[‡] Department of Materials Science, Fudan University, Shanghai 200433, PR China

*E-mail: sjding@fudan.edu.cn

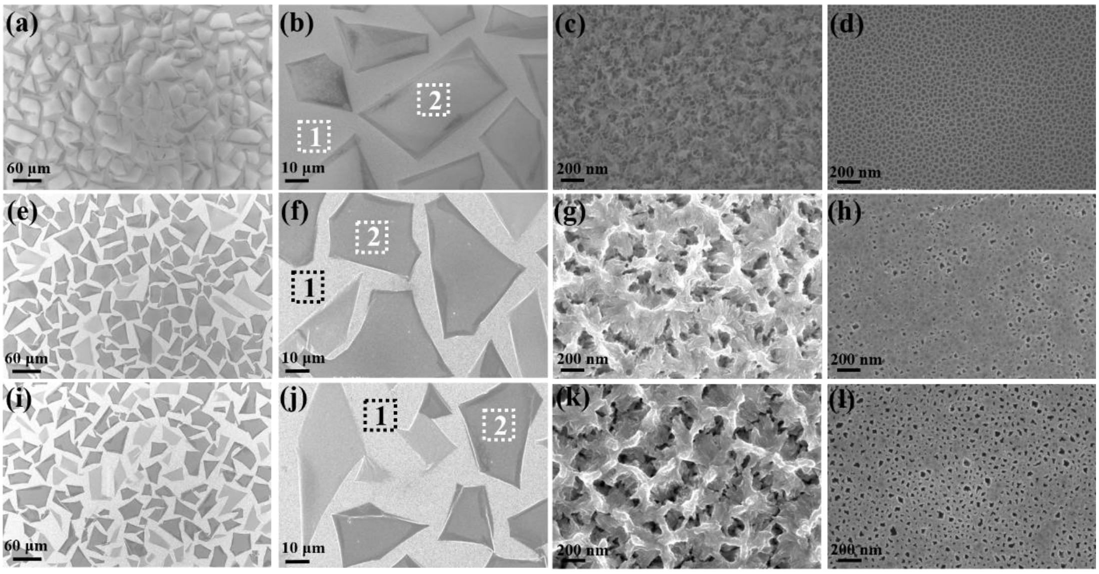

Figure S1. The planar SEM pictures of different samples: PS (a~d), PS/In_2O_3-51 (e~h) and PS/In_2O_3-85 (i~l). b, f and j are the magnified pictures of a, e and i. c and d are the magnified pictures of R1 and R2 marked in b. g and h are the magnified pictures of R1 and R2 marked in f. k and l are the magnified pictures of R1 and R2 marked in j.

Figure S1 shows the planar SEM pictures of PS (a~d), PS/In_2O_3-51 (e~h) and PS/In_2O_3-85 (i~l). Revealed in Figure S1(a), a large number of flake-like structures are observed. When a larger resolution is used, the flakes are confirmed as grooves，as shown in Figure S1(b). This indicates that the etching rate is not uniform on the whole silicon. Further zoom in the picture, the morphologies in the region 1(R1) and region 2(R2) marked in Figure S1(b) are different, displayed as Figure S1(c) and Figure S1(d), respectively. R2 is very flat with interconnected mesopores (20~50 nm). Instead, R1 exhibits rougher top morphology with porous structures. Since the Pt film is uniformly deposited on the silicon substrate, the different morphologies revealed in R1 and R2 are probably related to the etching process. When the silicon substrate was immersed into the etching solution, the Pt film within R1 was likely to crack and float in the solution due to the effect of capillary force from water and the one in R2 remained intact. In our previous research,[1] heavily doped mesoporous silicon (0.001~0.002 Ω·cm) was produced by Pt-nanoparticle assisted etching. It was found that mesopores were generated firstly on the whole substrate and then mesopores in direct contact with the Pt nanoparticles were continuously etched away. A similar etching behavior can be concluded in our case. The mesoporous layer emerged firstly in the overall silicon. Subsequently, the mesoporous layer in contact with the Pt film in R2 was readily to be etched and grooves were formed meanwhile. As the In_2O_3 films were coated, the contrast between R1 and R2 is much better, as shown in Figure S1(e, f, i and j). In addition, the introduction of In_2O_3 films results in much rougher top morphology for R1, revealed in Figure S1(g) and Figure S1(k). On the other hand, R2 is still flat with the addition of In_2O_3 films, shown in Figure S1(h) and Figure S1(l).

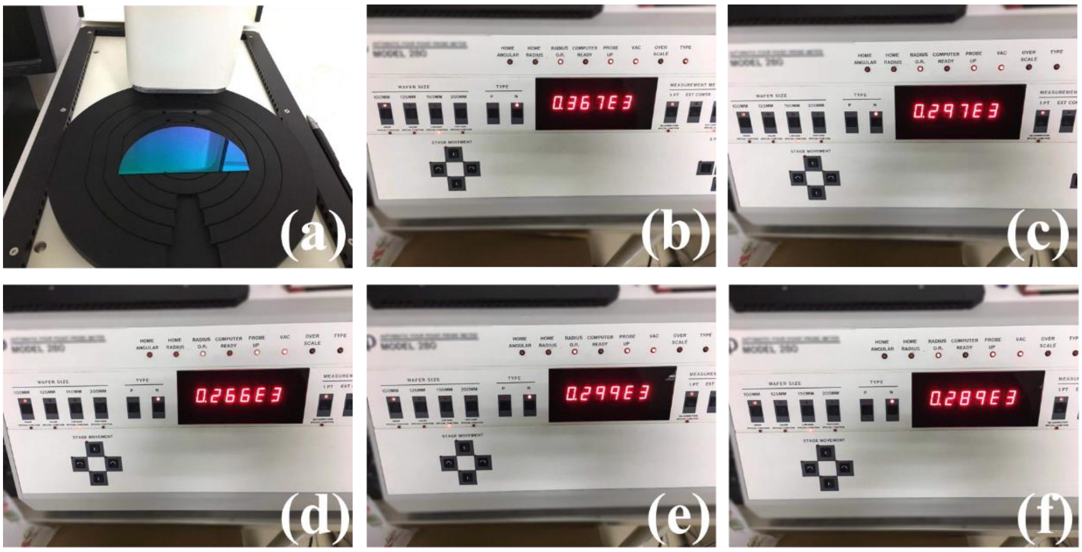

Figure S2. The optical picture of the four-point probe meter (a); the optical pictures of the sheet resistance values recorded at different points (b-f).

Table S1 The sheet resistance values recorded at different points.

Sheet resistance(Ω/□)	367	297	266	299	289
Average sheet resistance (Ω/□)	302				

In order to evaluate the conductivity of atomic layer deposited In_2O_3 films, 40-nm In_2O_3 films were grown on the SiO_2/Si substrate by ALD. SiO_2 was used to insulate the effect of the Si substrate. Then four-point probe meter was used to measure the sheet resistance of In_2O_3 films, as shown in Figure S2(a). Five points were selected to obtain the sheet resistance information (see Figure S2b-f) and the corresponding values were listed in Table S1. Since the average sheet resistance was 302 Ω/□, the average resistivity of In_2O_3 films was evaluated as ~0.0012 Ω·cm. Therefore, the atomic layer deposited In_2O_3 film has a higher conductivity.

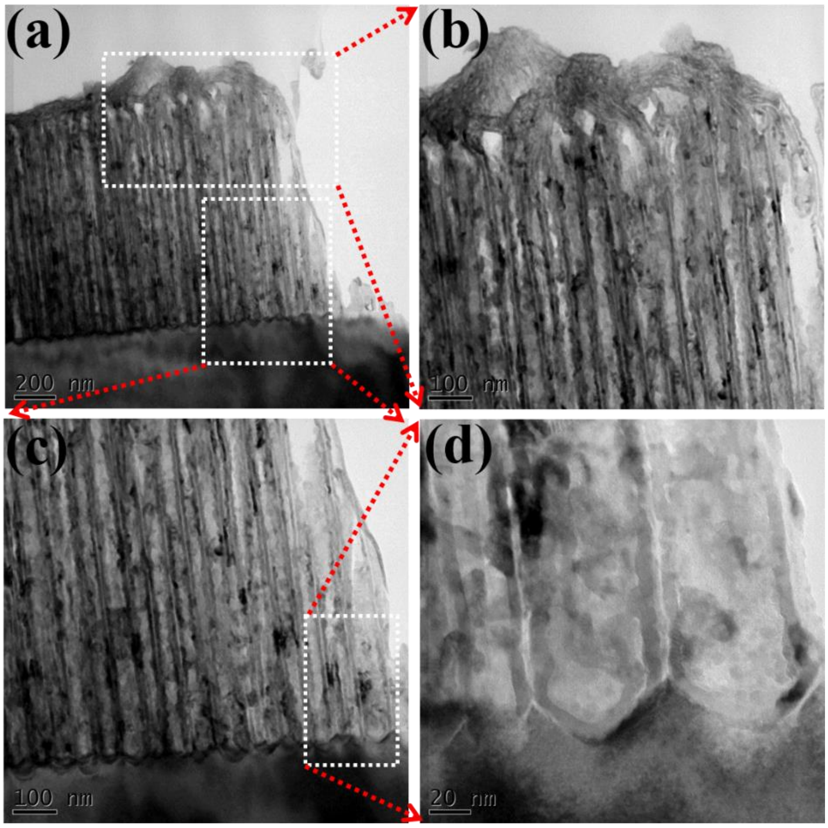

Figure S3. (a) The TEM picture of PS/In_2O_3-85 in R1; (b) the magnified picture of the marked area in (a); (c) the magnified picture of another marked area in (a); (d) the magnified picture of the marked area in (c).

In order to verify the uniformity, the TEM pictures of PS/In_2O_3-85 in R1 are provided, as shown in Figure S3. Figure S3(b) and (c) show the magnified pictures of the marked areas in Figure S3 (a) and the profile of the In_2O_3 films is clearly observed no matter in the top part or in the bottom part. Figure S3 (d) exhibits the magnified picture of the marked area in Figure S3 (c). It can be found that the In_2O_3 films are uniformly coated on the walls of the mesopores at the bottom.

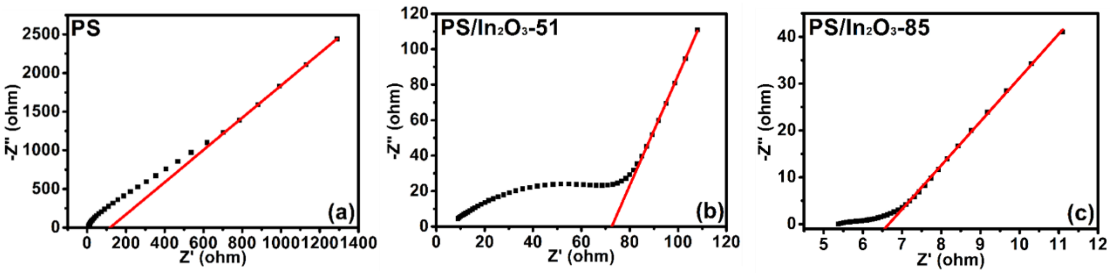

Figure S4. The EIS pictures in the high frequency range for PS (a); PS/In_2O_3-51 (b) and PS/In_2O_3-85 (c).

Figure S4 shows the EIS pictures of all the samples in the high frequency range. It can be found that there are semicircles in the high frequency range for PS and PS/In_2O_3-51. Instead, the semicircle is absent for PS/In_2O_3-85. The presence of a semicircle indicates the existence of redox reactions, which is consistent with the appearance of the redox peaks in the CV test for PS and PS/In_2O_3-51.

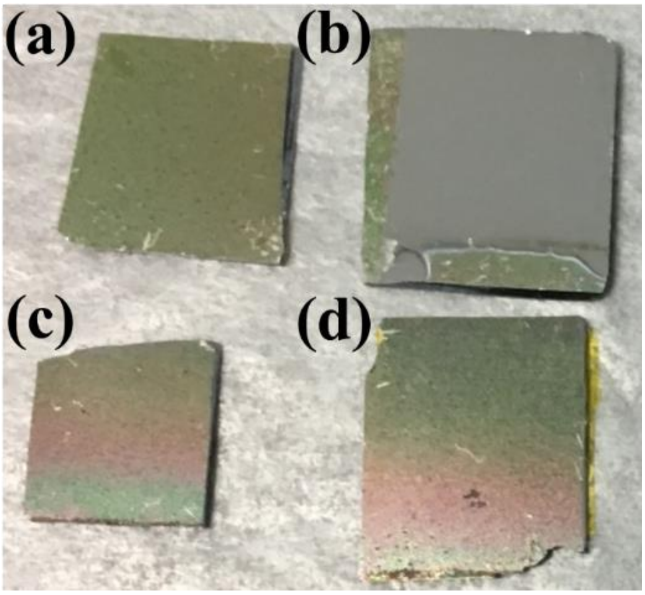

Figure S5. The optical pictures of PS without cyclic sweep (a) and with cyclic sweep (b); the optical pictures of PS/In_2O_3-51 without cyclic sweep (c) and with cyclic sweep (d).

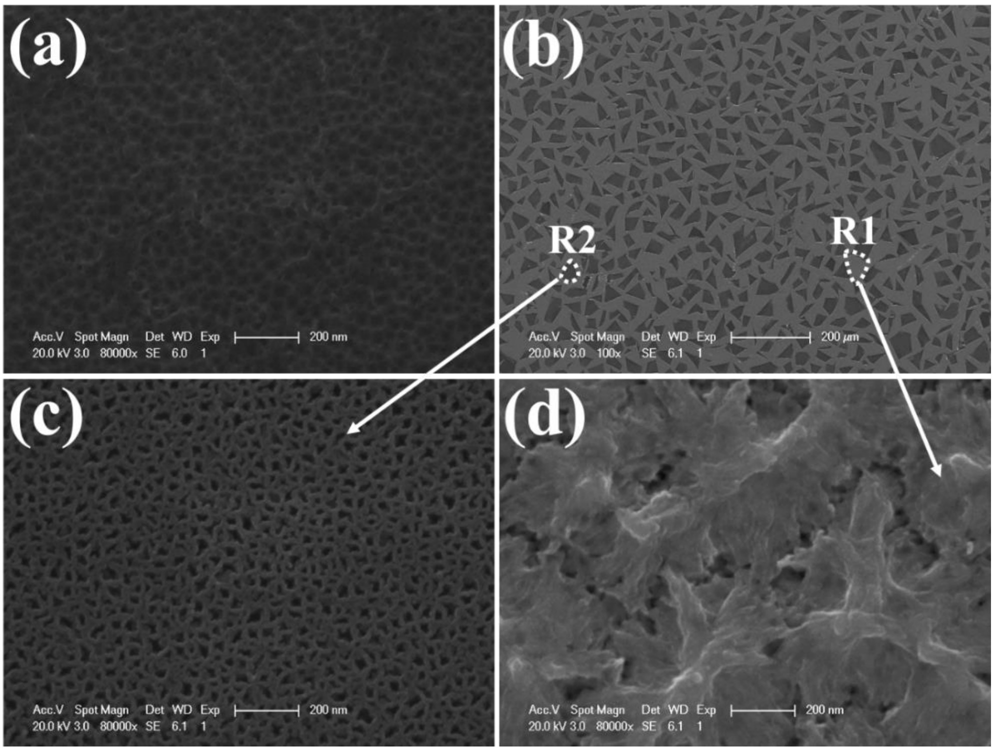

Figure S6. (a) The planar SEM picture of PS after cyclic sweep; (b) the planar SEM picture PS/In_2O_3-51 after cyclic sweep; (c) the enlarged picture of the marked area R2 in (b); (d) the enlarged picture of the marked area R1 in (b).

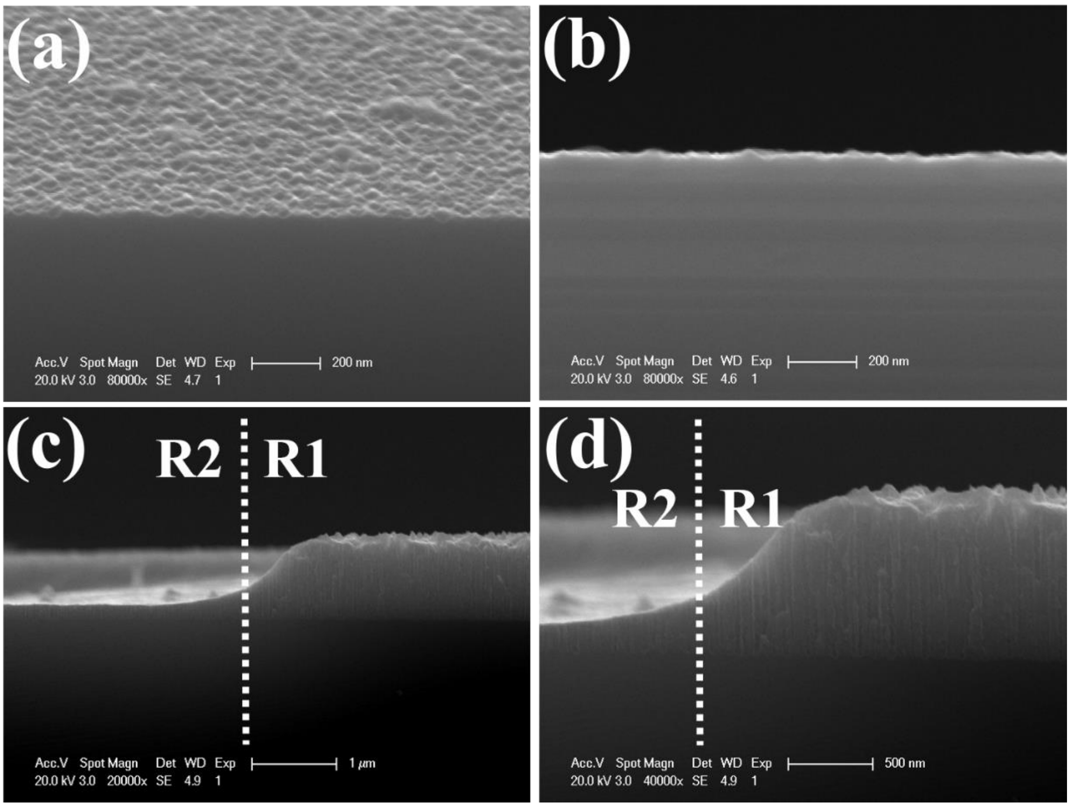

Figure S7. (a) The tilted SEM picture of PS after cyclic sweep; (b) the cross-section SEM picture of PS after cyclic sweep; (c) the cross-section SEM picture of PS/In_2O_3-51 after cyclic sweep; (d) the enlarged picture of R1 in (b).

As for the pristine PS sample, the capacitance density decreases with the number of cycles. Furthermore, it was found that something peeled off the sample and floated on the surface of the solution during the cyclic sweep. Figure S5(a) and (b) show the optical pictures of PS without and with cyclic sweep, respectively. It can be found that the color of the sample surface is changed after the cyclic sweep and is similar to that of the silicon substrate. Figure S6(a) displays the planar SEM picture of PS after cyclic sweep and a large number of cavities are observed. Figure S7(a) and (b) show the tilted and cross-section SEM pictures of PS after cyclic sweep, respectively. Likewise, only cavities are found on the substrate surface. These facts mean that PS was collapsed after cyclic sweep.

As for PS/In_2O_3-51 and PS/In_2O_3-85, the capacitance density increases abruptly during the first hundreds of cycles and then keeps constant. Figure S5(c) and (d) exhibit the optical pictures of PS/In_2O_3-51 without and with cyclic sweep, respectively and there is no obvious color change. Figure S6(b)-(d) display the planar SEM picture of PS/In_2O_3-51 after cyclic sweep and no obvious morphology variation is observed compared with that of the sample without cyclic sweep. As shown in Figure S7(c)-(d), the cross-section morphology is not changed too. These results indicate that the coating of In_2O_3 films enhances the structural stability of PS.

In a word, the pristine PS sample is readily collapsed during the cyclic sweep due to the irreversible redox reaction of silicon in the aqueous solution together with the volume expansion. With the coating of In_2O_3 films, reversible redox reaction or stable electric double layer will be existed between the In_2O_3 films and the electrolyte, thus enabling a stable cyclic sweep and enhancing the structural integrity.

REFERENCES

(1) Zhu, B.; Liu, W.-J.; Ding, S.-J.; Zhang, D. W.; Fan, Z. Formation Mechanism of Heavily Doped Silicon Mesopores Induced by Pt Nanoparticle-Assisted Chemical Etching. *J. Phys. Chem. C* **2018**, *122*, 21537-21542.